THE JOURNAL OF BIOLOGICAL CHEMISTRY
Vol. 280, No. 20, Issue of May 20, pp. 19569–19575, 2005

Printed in U.S.A.

Directed Evolution of Mammalian Cytochrome P450 2B1

MUTATIONS OUTSIDE OF THE ACTIVE SITE ENHANCE THE METABOLISM OF SEVERAL SUBSTRATES, INCLUDING THE ANTICANCER PRODRUGS CYCLOPHOSPHAMIDE AND IFOSFAMIDE*

Received for publication, January 5, 2005, and in revised form, March 15, 2005
Published, JBC Papers in Press, March 17, 2005, DOI 10.1074/jbc.M500158200

Santosh Kumar‡§, Chong S. Chen¶, David J. Waxman¶, and James R. Halpert‡

From the ‡Department of Pharmacology and Toxicology, University of Texas Medical Branch, Galveston, Texas 77555 and the ¶Department of Biology, Boston University, Boston, Massachusetts 02215

Cytochrome P450 2B1 has been subjected to directed evolution to investigate the role of amino acid residues outside of the active site and to engineer novel, more active P450 catalysts. A high throughput screening system was developed to measure H_2O_2-supported oxidation of the marker fluorogenic substrate 7-ethoxy-4-trifluoromethylcoumarin (7-EFC). Random mutagenesis by error-prone polymerase chain reaction and activity screening were optimized using the L209A mutant of P450 2B1 in an N-terminally modified construct with a C-terminal His tag (P450 2B1dH). Two rounds of mutagenesis and screening and one subcloning step yielded the P450 2B1 quadruple mutant V183L/F202L/L209A/S334P, which demonstrated a 6-fold higher k_{cat} than L209A. Further random or site-directed mutagenesis did not improve the activity. When assayed in an NADPH-supported reconstituted system, V183L/L209A demonstrated lower 7-EFC oxidation than L209A. Therefore, F202L/L209A/S334P was generated, which showed a 2.5-fold higher k_{cat}/K_m for NADPH-dependent 7-EFC oxidation than L209A. F202L/L209A/S334P also showed enhanced catalytic efficiency with 7-benzyloxyresorufin, benzphetamine, and testosterone, and a 10-fold increase in stereoselectivity for testosterone 16α- *versus* 16β-hydroxylation compared with 2B1dH. Enhanced catalytic efficiency of F202L/L209A/S334P was also retained in the full-length P450 2B1 background with 7-EFC and testosterone as substrates. Finally, the individual mutants were tested for metabolism of the anti-cancer prodrugs cyclophosphamide and ifosfamide. Several of the mutants showed increased metabolism via the therapeutically beneficial 4-hydroxylation pathway, with L209A/S334P showing 2.8-fold enhancement of k_{cat}/K_m with cyclophosphamide and V183L/L209A showing 3.5-fold enhancement with ifosfamide. Directed evolution can thus be used to enhance P450 2B1 catalytic efficiency across a panel of substrates and to identify functionally important residues distant from the active site.

Advances in x-ray crystallography, homology modeling, and site-directed mutagenesis have yielded crucial insights into the structural basis of cytochrome P450 catalytic efficiency, differential substrate specificity, stereo- and regioselectivity, and cooperativity (1–9). These studies have revealed that substrate binding and oxidation are influenced not only by active site residues but also by residues outside of the active site that play a significant role in initial substrate recognition, substrate access, and redox partner binding (3, 4, 8, 9).

P450 enzymes of the 2B sub-family are among the best studied from the standpoint of structure-function relationships. These enzymes metabolize many xenobiotics, including the anti-cancer drugs cyclophosphamide (CPA)[1] and ifosfamide (IFA) and environmental contaminants such as polychlorinated biphenyls (1, 10–12). Comparison of active site residues among P450 2B enzymes within and across species has led to several successful efforts to enhance and/or re-engineer their activities (2, 10, 13–15). However, the extension of these studies to identify functionally important non-active site residues is more problematic. One attractive approach is directed evolution, which has been successfully applied to the design of industrial biocatalysts for enhanced catalytic efficiency, stability, and versatility and for examining the molecular basis of enzyme functions (16–21). Recent studies with the bacterial enzyme P450BM3 have illustrated the potential of directed evolution for engineering new and more efficient P450s showing enhanced hydroxylation of unnatural alkane substrates up to 100-fold. The resulting mutant has 10 of the 11 substitutions outside of the active site (22–24). Moreover, although the P450BM3 mutant with enhanced activity was selected using one specific substrate, it also showed improved activity with other substrates. Xenobiotic-metabolizing mammalian cytochromes P450, with their generally broader substrate specificity than bacterial P450s, offer the possibility of even greater applications in industrial synthesis, medicine, and bioremediation. Recently, directed evolution of mammalian P450 1A2 in two independent studies yielded mutants with 5- and 10-fold enhanced catalytic efficiency with 7-methoxyresorufin and 2-amino-3,5-dimethylimidazo[4,5-*f*]quinoline, respectively (25, 26). The mutations in both cases were outside of the active site.

The present study tests the hypothesis that directed evolution can be used to enhance the activity of P450 2B1 while maintaining versatility. First, we established a sensitive and direct high throughput screening method for a highly expressed truncated form of P450 2B1 using H_2O_2-supported oxidation of the marker fluorogenic substrate 7-ethoxy-4-trif-

* This work was supported by the NIEHS Center Pilot Grant ES06676 (to S. K.), by NIEHS Center Grant ES06676 and NIH Grant ES03619 (to J. R. H.), NIH Grant CA49248 (to D. J. W.), and by the Superfund Basic Research Center at Boston University, NIH Grant 5 P42 ES07381. The costs of publication of this article were defrayed in part by the payment of page charges. This article must therefore be hereby marked "*advertisement*" in accordance with 18 U.S.C. Section 1734 solely to indicate this fact.

§ To whom correspondence should be addressed: Dept. of Pharmacology and Toxicology, University of Texas Medical Branch, 301 University Blvd., Galveston, TX 77555-1031. Tel.: 409-772-9677; Fax: 409-772-9642; E-mail: sakumar@utmb.edu.

[1] The abbreviations used are: CPA, cyclophosphamide; IFA, ifosfamide; 7-EFC, 7-ethoxy-4-trifluoromethylcoumarin; 7-BR, 7-benzyloxyresorufin; CPR, cytochrome P450 reductase; UTMB, University of Texas Medical Branch.

luoromethylcoumarin (7-EFC) followed by optimization of random mutagenesis using error-prone PCR. Mutants with enhanced catalytic activity were then tested with 7-EFC and five other P450 2B1 substrates in a standard reconstituted system using NADPH. The results suggest several residues that may be targeted for mutagenesis to enhance activities toward compounds of medicinal and environmental interest.

EXPERIMENTAL PROCEDURES

Materials—7-EFC and 7-BR were purchased from Molecular Probes, Inc. (Eugene, OR). Polymyxin B sulfate, CPA, and NADPH were bought from Sigma. [4-^{14}C]Testosterone was obtained from Amersham Biosciences. 4-Hydroperoxy-CPA was obtained from ASTA Pharma (Beilefeld, Germany). IFA was obtained from the Drug Synthesis and Chemistry Branch of the NCI, National Institutes of Health. Recombinant NADPH-cytochrome P450 reductase (CPR) and cytochrome b_5 (b_5) from rat liver were prepared as described previously (27). Oligonucleotide primers for PCR were either obtained from The University of Texas Medical Branch, (UTMB), Molecular Biology Core Laboratory (Galveston, TX) or from Sigma Genosys (Woodlands, TX). Error-prone PCR and ligation kits were obtained from Roche Applied Science, restriction enzymes from Invitrogen, and the GeneClean kit from BIO 101, Inc. (Vista, CA). Quick-change XL site-directed mutagenesis kit was obtained from Stratagene (La Jolla, CA). Nickel-nitrilotriacetic acid affinity resin was purchased from Qiagen (Valencia, CA). All other chemicals were of the highest grade available and were obtained from standard commercial sources.

Random Mutagenesis by Error-prone PCR and Construction of Mutant Libraries—The method used is a modification of standard PCR methods, designed to alter and enhance the natural error rate of the polymerase, and was essentially performed as described previously for P450BM3 (28). Initially, error-prone PCR, ligation, and transformation were standardized for P450 2B1dH L209A to obtain >1000 clones per PCR reaction by selecting suitable forward and reverse primers, restriction sites, ligation conditions, and transformation procedures. Subsequently, error-prone PCR was standardized to ensure a mutation rate of 1–2 bp per P450 cDNA essentially as described previously (28). This was accomplished by varying the concentrations of nucleotides, especially dCTP and dTTP, and the concentrations of $MnCl_2$ to give mutation frequencies from 0.11 to 2% (1–20 nucleotides per 1 kb) (28). Finally, libraries were generated using the various conditions, and the number of mutations per kb was estimated based upon an activity screen as described previously (29) followed by sequencing of the desired mutants.

In the final conditions, the forward and reverse primers were as follows: 5′-CAC AGG AAA CAG ACC ATG GCT CCC AGT ATC-3′ (forward) and 5′-CGG ATA TCA ATG GTG GTG ATG CCG AGC TGA GAA-3′ (reverse). The restriction sites used were PstI and EcoRV. PCR reactions using an error-prone PCR kit included 25 mM $MgCl_2$, 10 mM dCTP, 10 mM dTTP, and 2 mM each of dATP and dGTP. The overnight ligation kit was used to obtain >1000 transformants per ligation reaction using ~20% of the PCR products.

The P450 2B1dH mutant F202L/L209A/S334P was generated by quick change site-directed mutagenesis using V183L/F202L/L209A/S334P as template and 5′-TGC TCC ATT **GTG** TTT GGA GAG-3′ and 5′-CTC TCC AAA **CAC** AAT GGA-3′ as forward and reverse primers, respectively. Similarly, F202L and F202L/L209A were generated by site-directed mutagenesis using 2B1dH and L209A as templates, respectively, and 5′-CTG TTG GAG CTG **TTG** TAC CGG ACC TTT-3′ and 5′-AAA GGT CCG GTA **CAA** CAG CTC CAA CAG-3′ as forward and reverse primers, respectively. Nucleotides presented in bold represent the site of mutation.

Screening and Selection of P450 2B1dH L209A Random Mutants—Screening and selection of 2B1dH L209A random mutants were essentially done as described previously for P450BM3 with minor modifications (30). Liquid handling was performed using a multichannel robot Biomek 2000 (Beckman, Fullerton, CA). In brief, transformed *Escherichia coli* (DH5α) was grown in a 300-μl, V-shaped 96-well microplate containing 150 μl of LB media for 18–20 h at 30 °C on a microplate shaker. Next, 20 μl of the LB-grown cells were inoculated into a 300-μl, V-shaped 96-well microplate containing 180 μl of TB medium and grown for ~3 h until cell density reached A_{600} = 1–1.5. δ-Aminolevulinic acid and isopropyl 1-thio-β-D-galactopyranoside were then added to the cells to final concentrations of 80 and 240 μg/ml, respectively. The cells were then grown for 72 h at 30 °C on a microplate shaker. Cells were then harvested by centrifugation at 5000 × *g* for 10 min using an Allegra 25R microplate centrifuge (Beckman). The supernatant was removed by decanting, and the pellet was dried. The cells were resuspended in 150 μl of 0.1 M Hepes buffer, pH 7.4, in the presence of 0.5 mg/ml lysozyme.

Next, 50 μl of the substrate mixture (300 μM 7-EFC containing 4% methanol and 20 units/well polymyxin B sulfate) was incubated with 40 μl of whole cells for 5 min at room temperature. The background intensity was recorded at λ_{ex} = 405 nm and λ_{em} = 510 nm using a fluorescence microplate reader (Ascent Fluoroscan, Ramsey, MN). The reaction was initiated by the addition of 10 μl of H_2O_2 (10 mM final), and the formation of product was recorded at 2.5 min. Mutants with ≥2-fold higher activity than the average wild-type activity were sequenced at the UTMB Protein Chemistry Laboratory and were further characterized as described below.

Expression and Purification of Wild-type and Engineered Enzymes—P450s 2B1 and 2B1dH and their mutants were expressed as His-tagged proteins in *E. coli* TOPP3 and purified using a Ni-affinity column as described previously (31). Protein concentrations were determined using the Bradford protein assay kit (Bio-Rad). The specific contents were between 8 and 15 nmol of P450 per milligram of protein. Upon purification, the yield, purity, and stability of the mutant proteins were either similar to or higher than the respective wild-type enzymes (2B1 and 2B1dH).

H_2O_2-dependent 7-EFC O-Deethylation Assay—H_2O_2-supported enzyme activities were assayed as described previously with slight modifications (32). Substrate mixtures were prepared in 100 mM Hepes buffer, pH 7.4, with 2% as the final concentration of methanol (100 μl/well of a 96-well microplate). The substrate mixture was preincubated with 50 pmol of purified P450 enzyme at room temperature for 5 min. Reactions were initiated by the addition of H_2O_2 to 10 mM. After 5 min of incubation, the reactions were stopped by adding 340 units (50 μl) of catalase. Subsequently, 50 μl of 100 mM Hepes buffer, pH 7.4, was added prior to recording the fluorescence intensity at λ_{ex} = 405 nm and λ_{em} = 510 nm using an Accent fluorescence plate reader.

NADPH-dependent Enzyme Assays—7-EFC and 7-BR oxidation were assayed using a fluorescence method (4). Benzphetamine *N*-demethylation was measured using a colorimetric method (9). Testosterone hydroxylation was assayed by TLC using radiolabeled substrate (2). The reconstitution of P450 2B1 and 2B1dH with CPR and b_5 in the NADPH system was carried out at ratios of 1:4:2 (31) and included 10 μg of dilauroylphosphatidylcholine/100-μl reaction volume in the P450 2B1 sample only. The reconstitution system for assaying CPA and IFA metabolism included P450 and purified rat liver CPR in a 1:4 molar ratio (5 pmol of P450/0.1 ml of 0.1 M KP_i buffer, pH 7.4, containing 0.1 mM EDTA) and was devoid of lipid and b_5. CPA and IFA metabolism were assayed by high-performance liquid chromatography as described (10). Steady-state kinetic parameters for 7-EFC, testosterone, 7-BR, and benzphetamine were determined by regression analysis using Sigma Plot (Jandel, San Rafel, CA). The K_m value was determined using the Michaelis-Menten equation, whereas the S_{50} and n values were determined using the Hill equation. Kinetic analysis of CPA and IFA metabolism was carried out using Enzyme Kinetics version 0.44 software (Trinity Software, Inc.).

P450 2B1 Model—The 2B1 model was made essentially as described (2). In brief, the initial molecular model was constructed using the Insight II software package (Homology, Discover_3, Biopolymer and Builder from Molecular Simulations, Inc., San Diego, CA). The model was constructed based on the crystal structure of a ligand-bound P450 2B4 complex (PDB entry 1SUO) (8). The sequence of rat 2B1 was obtained from SwissProt (accession number P00176). The coordinates of the conserved residues were assigned based on the corresponding residues of the 2B4 complex by Homology/Insight II. The heme group was copied from 2B4 into the 2B1 model.

RESULTS

Directed Evolution of P450 2B1dH—The most critical step of directed evolution is to find a simple, economical and high throughput activity screen. A facile assay method was sought to circumvent steps involving CPR and b_5 by using an alternate oxygen donor such as H_2O_2, as reported previously for bacterial P450eryF (22). To maximize heterologous expression and subsequent purification, an N-terminally modified construct of P450 2B1 with a C-terminal His tag was used (P450 2B1dH). Several known substrates of 2B1dH (derivatives of quinoline and coumarin) were tested using H_2O_2 and cumene hydroperoxide as oxygen donors. The combination of 7-EFC with H_2O_2 was found to give the highest signal-to-noise ratio and good

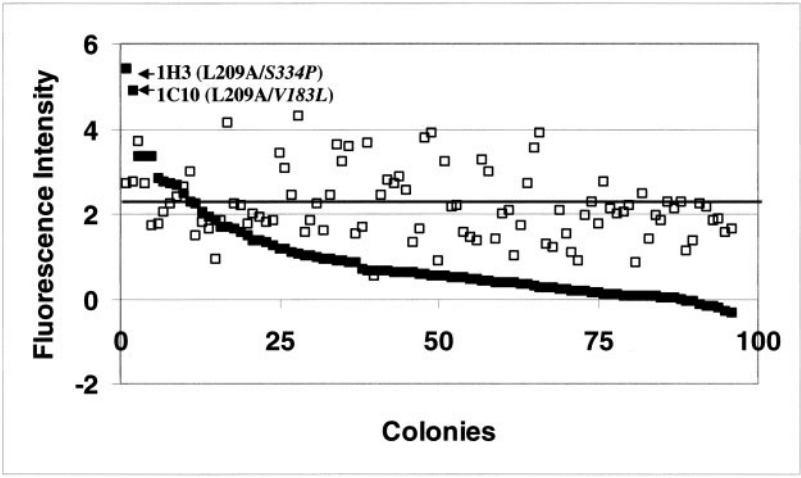

FIG. 1. **Screening of P450 2B1dH L209A random clones for the oxidation of 7-EFC.** *Open squares* represent the activities determined for individual clones of 2B1dH L209A and are plotted in random distribution of the activity to demonstrate the range across the 96-well microplate. The variation is ~80% from the mean (shown as a *horizontal line*). *Closed squares* represent the activities of individual clones of randomly mutagenized 2B1dH L209A and are plotted in decreasing order of activity. Approximately 30–40% clones have ≤10% of the average 2B1dH L209A activity (32). The *X*-axis represents individual colonies, and the *Y*-axis represents relative fluorescence intensity for the product, 7-HFC, at λ_{ex} = 405 nm and λ_{em} = 510 nm. The detailed methodology is described under "Experimental Procedures." Two high activity mutants of 2B1 L209A are marked as 1C10 and 1H3 (shown by *arrows*). These represent the site-specific mutants V183L and S334P, respectively.

reproducibility (data not shown). To further optimize the method, potassium phosphate, Tris-HCl, and Hepes buffer were tested in the absence and presence of $MgCl_2$; Hepes buffer without $MgCl_2$ gave maximal activity. H_2O_2-supported 7-EFC *O*-deethylation proceeded at ~5% the rate of the NADPH-supported activity under optimal conditions with purified 2B1dH (data not shown) (4). The H_2O_2-supported activity correlated well with the activity determined using NADPH across a panel of more than 10 active site mutants (Refs. 4 and 9 and data not shown).

2B1dH L209A had 10-fold higher H_2O_2-supported 7-EFC deethylation activity than 2B1dH and was therefore used as the starting template for directed evolution. In adapting the assay to bacterial cells grown on microtiter plates, a number of difficulties were encountered, including high background, low activity, and variable expression. Improvements were obtained by eliminating imidazole from the TB culture medium, using whole cells in place of cell extracts, and using 300 μl of V-shaped 96-well microplates instead of 1-ml deep well microplates. A representative assay of multiple colonies of 2B1dH L209A indicated ~80% colony-to-colony variation in activity (Fig. 1, *open squares*) compared with the average 2B1dH L209A colony (Fig. 1, *horizontal line*). These data suggested that random clones having ≥2-fold higher activity than 2B1dH L209A would correspond to mutants with enhanced catalytic activity.

Identification of 2B1dH Mutant V183L/F202L/L209A/S334P with a 6-fold Increased k_{cat}—Representative data from an initial screen of several hundred random clones derived by directed evolution of 2B1dH L209A are shown in Fig. 1, with the clones graphed in order of decreasing activity (*closed squares*). Two of the clones (1H3 and 1C10) showed activity of ≥2-fold higher than the average of 2B1dH L209A, and higher than any single 2B1dH L209A colony. DNA sequencing revealed a single new mutation in each case, S334P (clone 1H3) and V183L (clone 1C10). V183L/L209A and L209A/S334P were expressed in large scale culture and purified. Both showed similar expression levels as 2B1dH, as reported earlier for L209A (4). L209A/S334P and V183L/L209A had 50–58% higher k_{cat} values than L209A (Table I). In an effort to enhance the activity further, the triple mutant V183L/L209A/S334P was prepared. This mutant displayed ~2-fold higher k_{cat} than L209A (Table I).

Directed evolution using V183L/L209A/S334P as the template yielded V183L/F202L/L209A/S334P. This quadruple mutant had a 3-fold higher k_{cat} than V183L/L209A/S334P and 6-fold higher k_{cat} than L209A, along with an increased S_{50} and an n value of 1.6 (Table I). A third round of mutagenesis and screening did not yield any colonies with a further ≥2-fold increase in activity. Five of the most active clones were sequenced, which identified only one clone with an additional mutation, E322K. Purified V183L/F202L/L209A/E322K/S334P showed no further enhancement of k_{cat}, suggesting that random mutagenesis was approaching saturation for enhanced 7-EFC *O*-deethylation (data not shown). We therefore sought a rational mutagenesis approach in an effort to achieve higher activity. Of several 2B1dH active site mutants (V103A, V103I, I114A, L208A, L220A, S221P, I290A, and I290F) available from earlier studies (2, 4, 9) that showed higher NADPH-dependent activity, I290F showed 3-fold higher H_2O_2-dependent activity than 2B1dH (data not shown). However, V183L/F202L/L209A/I290F/S334P showed no increase in k_{cat} beyond V183L/F202L/L209A/S334P (data not shown), again suggesting saturation of activity along this particular directed evolution pathway.

TABLE I
Steady-state kinetics: H_2O_2-dependent oxidation of 7-EFC by P450 2B1dH L209A and its mutants

Results are the mean ± standard deviation of three independent experiments. 2B1dH showed very low activity (~0.2 min^{-1} at 150 μM 7-EFC), and kinetic parameters could not be determined.

Sample	k_{cat}	S_{50}	n
	min^{-1}	μM	
L209A	1.2 ± 0.1	12 ± 2.0	1.2 ± 0.1
L209A/S334P	1.8 ± 0.1	17 ± 3.2	0.9 ± 0.1
V183L/L209A	1.9 ± 0.1	14 ± 3.1	0.8 ± 0.1
V183L/L209A/S334P	2.3 ± 0.2	18 ± 2.0	1.0 ± 0.1
V183L/F202L/L209A/S334P	7.2 ± 0.2	36 ± 1.4	1.6 ± 0.2

F202L/L209A/S334P Demonstrates the Highest Catalytic Efficiency of NADPH-dependent 7-EFC O-Deethylation—Subsequently, the 2B1dH mutants were assayed in a standard reconstituted system using NADPH. Compared with 2B1dH L209A, L209A/S334P had 37% higher k_{cat}/K_m, whereas V183L/L209A had a ~20% lower k_{cat}/K_m (Table II). Adding F202L to V183L/L209A/S334P increased the k_{cat}/K_m for 7-EFC ~2-fold,

TABLE II
Steady-state kinetics: NADPH-dependent oxidation of 7-EFC by 2B1dH L209A and its mutants

Results are the mean ± S.D. of three independent experiments.

Sample	k_{cat}	K_m	k_{cat}/K_m
	min^{-1}	μM	
2B1dH[a]	12 ± 0.4		
L209A	35 ± 0.73	18 ± 2.1	1.9
L209A/S334P	44 ± 1.6	17 ± 1.8	2.6
V183L/L209A	23 ± 0.86	15 ± 1.8	1.5
V183L/L209A/S334P	24 ± 0.61	11 ± 1.5	2.2
V183L/F202L/L209A/S334P	52 ± 4.0	12 ± 1.6	4.3
F202L/L209A/S334P	77 ± 1.7	16 ± 1.3	4.8

[a]Activity of 2B1dH follows the Hill equation with an n value of 1.7 and S_{50} of 23 μM.

whereas incorporation of E322K did not enhance the activity further (Table II, data not shown). Interestingly, V183L/F202L/L209A/S334P did not show cooperativity in the NADPH-dependent system (data not shown). In contrast to the H_2O_2-supported activity, incorporation of I290F into V183L/F202L/L209A/S334P decreased the k_{cat}/K_m by ~25% in the NADPH-dependent system (data not shown). Because V183L decreased NADPH-supported activity, this mutation was removed from V183L/F202L/L209A/S334P. The resulting triple mutant F202L/L209A/S334P showed the highest k_{cat}/K_m (~2.5-fold higher than L209A) of all samples tested (Table II). As expected, F202L/L209A/S334P showed slightly lower activity than V183L/F202L/L209A/S334P in the H_2O_2-supported system (data not shown).

F202L/L209A/S334P Exhibits Enhanced Oxidation of Several Other Substrates—The 2B1dH random mutants were tested with 7-BR, benzphetamine, and testosterone to investigate whether the enhanced NADPH-dependent activity was retained across structurally diverse substrates (Fig. 2). Testosterone 16α-hydroxylation paralleled NADPH-supported 7-EFC oxidation across the panel of mutants. As expected, F202L/L209A/S334P showed the highest activity (Fig. 2), along with >10-fold increase in stereoselectivity for testosterone 16α- over 16β-hydroxylation. With 7-BR as substrate, the relative activities of the mutants were somewhat different from 7-EFC and testosterone, and V183L/F202L/L209A/S334P showed higher activity than F202L/L209A/S334P (Fig. 2). The relative activities of the mutants with benzphetamine were very different from the other substrates. Although most of the mutations had little or no effect on benzphetamine metabolism, F202L/L209A/S334P showed ~2-fold higher activity than 2B1dH or 2B1dH L209A (Fig. 2).

Steady-state kinetic analysis of the oxidation of testosterone, 7-BR, and benzphetamine was performed with 2B1dH and three of the mutants (Table III). Although V183L/F202L/L209A/S334P showed the highest activity at saturating 7-BR concentration, F202L/L209A/S334P showed the highest k_{cat}/K_m (~3-fold higher than L209A) due in part to a ~2-fold decrease in K_m value. Relative to L209A, F202L/L209A/S334P showed a ~4-fold improved k_{cat}/K_m with benzphetamine and 1.7-fold improved k_{cat}/K_m for testosterone 16α-hydroxylation. Thus, F202L/L209A/S334P showed enhanced catalytic efficiency with four structurally distinct substrates.

F202L/L209A/S334P Demonstrates Enhanced Catalytic Activity When Incorporated into Full-length 2B1—The next step was to test whether the enhanced activity of F202L/L209A/S334P seen in the 2B1dH (N-terminal deleted) background was manifest when introduced into full-length 2B1. Results of kinetic analysis of 2B1 F202L/L209A/S334P with 7-EFC, 7-BR, benzphetamine, and testosterone are shown in Table IV. F202L/L209A/S334P showed a k_{cat}/K_m value that was >20-fold higher than full-length 2B1 for testosterone 16α-hydroxylation.

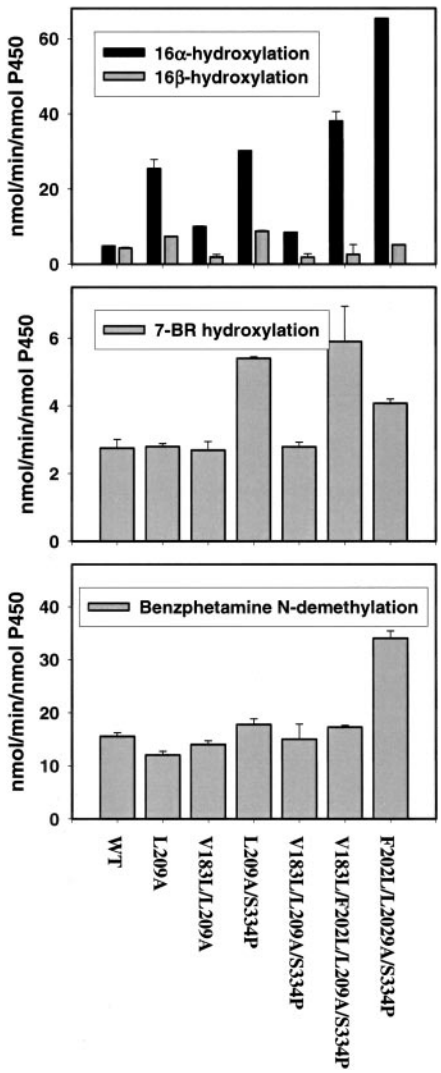

FIG. 2. **Testosterone and 7-BR hydroxylation and benzphetamine *N*-demethylation catalyzed by 2B1dH and its mutants.** Metabolism of testosterone (*top panel*), 7-BR (*middle panel*), and benzphetamine (*bottom panel*) were measured at 200, 8, and 500 μM substrate concentrations, respectively. *Bars* represent mean values ± half-the range based on two independent determinations.

The stereoselectivity for testosterone 16α-hydroxylation was also increased by 10-fold. F202L/L209A/S334P catalyzed testosterone 16α-hydroxylation with a k_{cat} (150 min^{-1}) that is among the highest reported for any mammalian cytochrome P450 in an NADPH-supported reaction. F202L/L209A/S334P did not show enhanced catalytic efficiency for 7-BR or benzphetamine oxidation, perhaps reflecting the different phospholipid dependences of full-length *versus* truncated P450 2B1 and the proximity of residues 202 and 209 to a proposed secondary lipid binding site (33).

Role of F202L in Substrate Metabolism—Analysis of the above described mutants suggested that F202L may contribute significantly to the enhanced enzyme activity seen with several substrates. Therefore, kinetic analysis was performed with F202L and F202L/L209A in the 2B1dH background (Table V). Surprisingly, F202L showed decreased activity with 7-EFC in the H_2O_2-supported reaction compared with 2B1dH. In addition, F202L showed a decreased k_{cat} for the oxidation of 7-EFC and 7-BR, and for testosterone 16α-hydroxylation compared with 2B1dH (Tables II and III *versus* Table V). Compared with L209A, F202L/L209A showed enhancement in the k_{cat} by 2.5-fold for 7-EFC deethylation in the H_2O_2-supported reaction

TABLE III
Steady-state kinetics of 2B1dH and its mutants: NADPH-dependent oxidation with various substrates
Results are the representative of at least two independent determinations. The variation between the experiments is ≤10%.

	7-BR			Benzphetamine			Testosterone 16α -OH		
	k_{cat}	K_m	k_{cat}/K_m	k_{cat}	K_m	k_{cat}/K_m	k_{cat}	K_m	k_{cat}/K_m
	min^{-1}	μM		min^{-1}	μM		min^{-1}	μM	
2B1dH	3.5 (0.3)[a]	2.5 (0.5)	1.4	15 (1.0)	44 (7)	0.34	4.1 (1.0)	29 (4.0)	0.14
L209A	3.6 (0.1)	1.5 (0.2)	2.4	11 (1.0)	40 (6)	0.27	31 (1.4)	31 (4.5)	1.0
V183L/F202L/L209A/S334P	5.6 (0.2)	1.3 (0.1)	4.3	14 (1.1)	92 (12)	0.15	36 (1.5)	32 (4.7)	1.1
F202L/L209A/S334P	4.2 (0.1)	0.61 (0.1)	6.8	37 (2.2)	33 (6)	1.1	69 (6.2)	40 (5.7)	1.7

[a] Standard errors for fit to Michaelis-Menten are shown in parenthesis.

TABLE IV
Steady-state kinetics of full-length 2B1 and 2B1 F202L/L209A/S334P: NADPH-dependent oxidation with various substrates
Results are the representative of at least two independent determinations. The variation between the experiments is ≤10%.

Substrate	2B1			2B1 F202L/L209A/S334P		
	k_{cat}	K_m	k_{cat}/K_m	k_{cat}	K_m	k_{cat}/K_m
	min^{-1}	μM		min^{-1}	μM	
7-EFC[a]	21 (0.62)[b]			55 (2.5)	15 (1.5)	3.8
7-BR	3.1 (0.20)	1.2 (0.20)	2.6	2.6 (0.2)	0.8 (0.2)	3.2
Benzphetamine	62 (3.2)	66 (10)	0.93	76 (5.0)	98 (17)	0.77
Testosterone 16α-OH	11 (1.1)	33 (7.0)	0.33	150 (20)	21 (6)	7.1
Testosterone 16β-OH	11 (1.0)	35 (5.0)	0.31	15 (2.1)	23 (7)	0.65

[a] 7-EFC oxidation for the 2B1 enzyme follows the Hill equation with an n value of 1.4 and S_{50} of 62 μM.
[b] Standard errors for fit to the Michaelis-Menten or Hill equation are shown in parenthesis.

TABLE V
Steady-state kinetics of 2B1dH F202L and F202L/L209A: NADPH-dependent oxidation of various substrates
Results are the representative of at least two independent determinations. The variation between the experiments is ≤10%.

Substrate	F202L			F202L/L209A		
	k_{cat}	K_m	k_{cat}/K_m	k_{cat}	K_m	k_{cat}/K_m
	min^{-1}	μM		min^{-1}	μM	
7-EFC[a]	-[b]			3.3[c] (0.3)[d]		
7-EFC	8.7 (0.54)	30 (5.4)	0.29	48 (1.4)	13 (1.2)	3.7
7-BR	2.0 (0.2)	0.87 (0.2)	2.3	3.6 (0.2)	0.80 (0.2)	4.5
Testosterone 16α-OH	3.6 (0.24)	126 (16)	0.03	65 (1.9)	43 (3.6)	1.5

[a] 7-EFC oxidation was measured using the H_2O_2 system.
[b] F202L showed very low activity (0.11 min^{-1} at 150 μM 7-EFC), and kinetic parameters could not be determined.
[c] 7-EFC oxidation for F202L/L209A follows the Hill equation with an n value of 1.2 and S_{50} of 23 μM.
[d] Standard errors for fit to the Michaelis-Menten or Hill equation are shown in parenthesis.

(Table I *versus* V). In addition, compared with L209A, F202L/L209A showed 1.5- to 1.9-fold enhanced k_{cat}/K_m for the oxidation of 7-EFC and 7-BR, and for testosterone 16α-hydroxylation in the standard reconstituted system (Tables II and III *versus* Table V). F202L/L209A also showed enhanced stereoselectivity by >14-fold for testosterone 16α- *versus* 16β-hydroxylation compared with 2B1dH (data not shown).

2B1dH Mutants L209A/S334P and V183L/L209A, Respectively, Show Enhanced Catalytic Efficiency for CPA and IFA 4-Hydroxylation—Finally, selected P450 2B1 mutants were tested for improved catalytic properties toward the anti-cancer prodrugs CPA and IFA, as judged by decreases in K_m, increases in k_{cat} for 4-hydroxylation (drug activation), or decreases in k_{cat} for *N*-dechloroethylation, an undesirable toxic side-reaction. Initial studies revealed that 2B1dH showed a 3-fold decrease in K_m for both CPA and IFA (Fig. 3) compared with full-length 2B1, without a significant change in k_{cat} (10). Moreover, each of the 2B1dH mutants showed a 2- to 3-fold further decrease in K_m for CPA compared with 2B1dH (Fig. 3), as well as 3- to 7-fold decreases in k_{cat} for CPA *N*-dechloroethylation (data not shown). However, only L209A/S334P showed an enhanced k_{cat} for CPA 4-hydroxylation. The catalytic efficiency of L209A/S334P for CPA 4-hydroxylation was improved 2.8-fold over 2B1dH and represents the highest value observed to date (220 min^{-1} mM^{-1}) for this reaction by a mammalian P450.

With IFA as substrate, k_{cat} and k_{cat}/K_m for the 4-hydroxylation reaction were the highest for V183L/L209A (Fig. 3). F202L/L209A/S334P also exhibited an elevated k_{cat} compared with 2B1dH, but the K_m of that triple mutant was also elevated, such that there was no overall improvement in catalytic efficiency. The other 2B1dH mutants had k_{cat} values similar to L209A and slightly increased over 2B1dH. The overall improvement in the catalytic efficiency of V183L/L209A and V183L/F202L/L209A/S334P was ~2.5- to 3-fold over 2B1dH. V183L/L209A and V183L/F202L/L209A/S334P are the most efficient among the 2B1 mutant enzymes for IFA 4-hydroxylation (k_{cat}/K_m ~50–70 min^{-1}, mM^{-1}). Finally, all the mutants showed significantly decreased IFA *N*-dechloroethylation (61% metabolism of IFA via the *N*-dechloroethylation pathway for 2B1dH *versus* 41–47% IFA *N*-dechloroethylation by each of the mutants; data not shown).

DISCUSSION

As a complement to extensive prior site-directed mutagenesis, homology modeling, and x-ray crystallographic studies, we developed a directed evolution approach for mammalian xenobiotic-metabolizing cytochromes P450 2B. A major goal was to identify non-active site substitutions that might enhance activity across a panel of structurally diverse substrates, as seen earlier in bacterial P450BM3, in which random mutagenesis yielded 10 of the 11 beneficial mutations in non-active site regions (23). Development of this approach with P450 2B1 was greatly facilitated by the availability of 2B1dH L209A, which shows 10-fold higher heterologous expression and a 2-fold

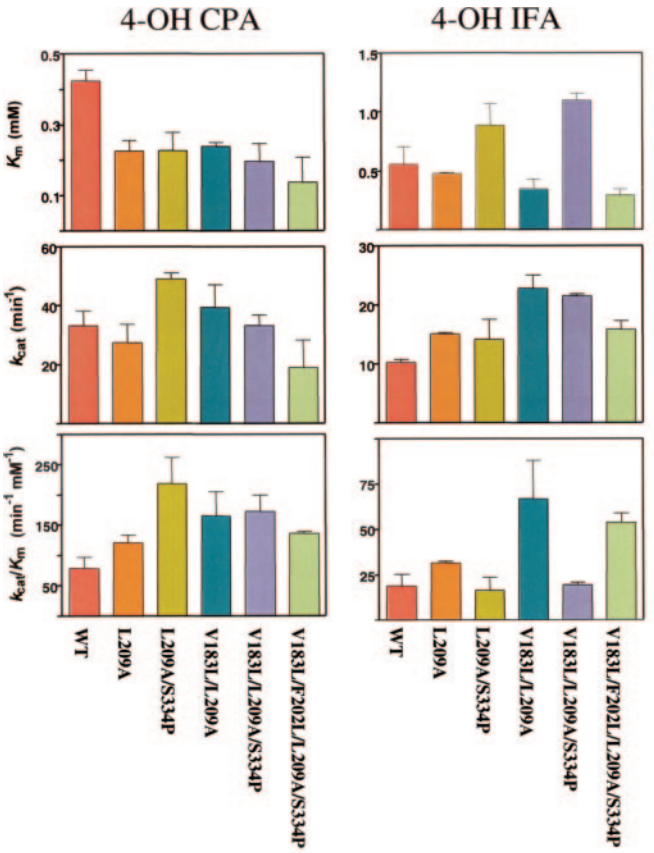

FIG. 3. **Steady-state kinetics of CPA and IFA 4-hydroxylation.** 4-Hydroxylase activities were determined for CPA (*left set of panels*) and for IFA (*right set of panels*) as described under "Experimental Procedures." The *Y*-axis displays K_m, k_{cat}, and k_{cat}/K_m, values, and the *X*-axis presents the individual mutants. *Bars* represent mean values ± half-the range based on two independent determinations. Note differences in *y*-axis scales for CPA and IFA.

higher k_{cat} for 7-EFC *O*-deethylase activity than full-length 2B1 (4, 31). Two rounds of directed evolution and one subcloning step yielded 2B1dH V183L/F202L/L209A/S334P, which exhibited a 6-fold enhanced k_{cat} for 7-EFC metabolism in an H_2O_2-supported reaction. Elimination of the V183L mutation, which proved deleterious for 7-EFC metabolism supported by NADPH in a standard reconstituted system, yielded a triple mutant, F202L/L209A/S334P, which displayed 3- to 4-fold enhanced catalytic efficiency toward 7-BR, benzphetamine, and testosterone. This triple mutant also retained enhanced catalytic efficiency with 7-EFC and testosterone in the full-length 2B1 background. One advantage of directed evolution from the standpoint of generating novel catalysts for biomedical or bioengineering applications is that only mutants with good expression levels and stability are isolated in the whole cell screens. In contrast, mutagenesis targeted to the active site often yields mutants with decreased expression and/or stability, especially when multiple substitutions are combined (2).

Although, 2B1dH V183L/F202L/L209A/S334P and F202L/L209A/S334P exhibited enhanced catalytic efficiency with several substrates, some interesting differences in function were also observed, including differences between H_2O_2- and NADPH-dependent 7-EFC *O*-deethylation, NADPH-dependent oxidation of one substrate *versus* another substrate (*e.g.* IFA *versus* CPA), and catalytic activity of 2B1dH *versus* full-length 2B1. Clearly these differences reflect the location of the mutated residues in the three-dimensional structure of the protein. Although no x-ray crystal structure of P450 2B1 is available, the recently solved structure of an inhibitor-bound form of P450

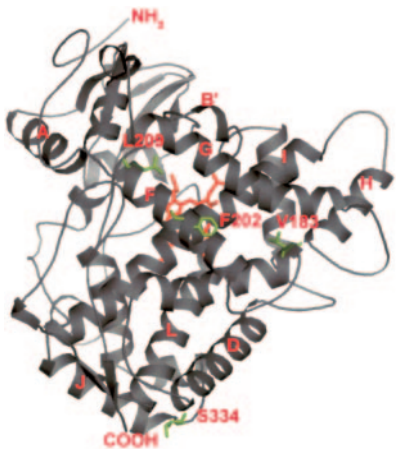

FIG. 4. **2B1 model based on the crystal structure of 2B4.** The heme (*red sticks*) and residues where mutations were found (*green sticks*) are shown. The position of helices and the N and C termini are also labeled.

2B4 (8) provides the best possible template for homology modeling (Fig. 4). Two of the three 2B1 mutations (V183L and S334P) map to regions of the protein distant from the active site. Residue 183 is located in the E-helix (near SRS 2) and has not previously been implicated in P450 function. More recently, random mutagenesis of P450 1A2 generated a Val^{193} → Met mutation, which may contribute to enhanced oxidation of 7-methoxyresorufin (26). Residue 193 is presumed to be located in the E-helix, suggesting an important functional role of this region. Although, V183L/L209A did not show enhanced activity in the NADPH-dependent system with most of the substrates tested, it showed enhanced catalytic efficiency and increased regioselectivity for IFA 4-hydroxylation. The enhanced H_2O_2-dependent but diminished NADPH-dependent 7-EFC *O*-deethylase activity of V183L/L209A relative to L209A is also intriguing and suggests impairment of the interaction with redox partners (CPR and/or b_5), leading to a decrease in hydroperoxy complex formation. The other important residue identified here, Ser^{334}, is located in the J-J′ loop (between substrate recognition sites 5 and 6), and also has not been implicated previously in P450 function. Interestingly, introduction of S334P enhanced catalytic efficiency with all the substrates tested in the NADPH-dependent system. The presence of Pro at the same position in P450 2B11 may contribute to its high catalytic efficiency and regioselectivity for CPA 4-hydroxylation (*cf.*, Ref. 10). Analysis of long range effects of residues 183 and 334 as described by Hilser and colleagues may shed light on some of these observations (34, 35).

Although, Phe^{202} → Leu is deleterious for 2B1 activity with several substrates, the addition of F202L to L209A or to V183L/L209A/S334P enhanced catalytic activity. In addition, inclusion of F202L increased the stereoselectivity of testosterone 16α-hydroxylation (Fig. 2), as was observed for L209A (4). Based on earlier mutagenesis work, this region of the protein is important for substrate binding, substrate specificity, and stereo- and regioselectivity in P450 2B and P450 2C enzymes (2, 4, 33). Amino acids 201–210 have been proposed to form a secondary lipid binding site in P450 2C5 and 2C3 (33). In particular, residues 201, 202, and 205 contribute to the differences in catalytic activity between P450 2C5 and 2C3 and in the lipid dependence of the two enzymes. Therefore, it is likely that due to different lipid requirements, the Phe^{202} → Leu mutation leads to differences in activity between truncated and full-length 2B1 F202L/L209A/S334P for 7-BR and benzphetamine oxidation.

Based on the 4-(4-chlorophenyl)imidazole-bound 2B4 struc-

ture (8), and a 2B1 model docked with testosterone (data not shown), Phe^{202} is outside of the active site (distance from the substrate > 8.0 Å). Residue Leu^{209} in 2B1 and 2B4 is ≤5.0 Å from the substrate in the active site. $Phe^{202}$and Leu^{209} may also be critically important residues for making the 15-Å open cleft between helices F and G, as seen in the substrate-free P450 2B4 structure. This open cleft has been proposed to control the entry of a diverse array of substrates (3, 8). Based on the prediction from the P450 2B4 crystal structure and our overall data it appears that helix F and the F′ region are critical for enzyme activity, substrate specificity, stereo- and regioselectivity, and enzyme cooperativity. Therefore, a more targeted mutagenesis approach in this region may be very fruitful.

Our observations with specific mutants are interesting from the standpoint of developing an improved P450 2B enzyme for use in activating the anti-cancer prodrugs CPA and IFA in the context of gene therapy treatment for cancer (36, 37). At present, P450 2B11 is the most efficient catalyst of CPA and IFA activation, which proceeds via 4-hydroxylation. Earlier efforts to improve the catalytic efficiency of P450 2B1 with CPA and IFA revealed that 2B1 mutants I114V and I114V/V363I have a ~2-fold enhanced k_{cat}/K_m for CPA and IFA 4-hydroxylation, respectively (10). These results prompted the investigation of 2B11, which has Val^{114} and Leu^{363}. Interestingly, 2B1dH V183L/L209A and L209A/S334P, generated by directed evolution, not only showed ~3-fold enhanced catalytic efficiency for activation of the prodrug substrates IFA and CPA, respectively, but also increased regioselectivity for metabolism via the 4-hydroxylation pathway. Given the ~2-fold decrease in K_m for CPA 4-hydroxylation seen with all of the L209A-containing 2B1 mutants examined (Fig. 3), introduction of the $Leu^{209} \rightarrow Ala$ substitution into 2B11 may lead to a corresponding decrease in K_m and an increase in catalytic efficiency and/or regioselectivity for CPA 4-hydroxylation.

In summary, our results demonstrate that directed evolution of P450 2B1 can be used to identify critical amino acid substitutions and combinations of substitutions outside of the active side that are unlikely to be identified or predicted from x-ray crystal structures. The mutants described here showed high expression and stability along with enhanced catalytic efficiency toward multiple substrates. This study should facilitate further design of P450s for synthetic, medical, and environmental applications. This approach may also be utilized for random mutagenesis of P450 2B1 in the F-G region, and may be applied to other mammalian P450s of medical or industrial importance.

Acknowledgments—We thank Drs. Frances Arnold and Edgardo Farinas from California Institute of Technology for providing technical details of directed evolution and sharing their unpublished materials. We thank Drs. Kenneth Johnson and Cheng Wang, Pharmacology and Toxicology, UTMB, for use of their fluorescence plate reader. We thank Dr. Hong Liu for generating the 2B1 model, You-Qun He for technical support in optimizing error-prone PCR, and Lisa Sun for making the F202L and F202L/L209A mutants. We also thank Jeeba Kuriakose and Alva Gullstrand for assistance during their Summer Undergraduate Research Program. Finally, we thank the NIEHS Center, National Institutes of Health, UTMB for providing start-up money to initiate this research.

REFERENCES

1. Domanski, T. L., and Halpert, J. R. (2001) *Curr. Drug Metab.* **2,** 117–137
2. Kumar, S., Scott, E. E., Liu, H., and Halpert, J. R. (2003) *J. Biol. Chem.* **278,** 17178–17184
3. Scott, E. E., He, Y. A., Wester, M. R., White, M. R., Chin, C. C., Halpert, J. R., Johnson, E. F., and Stout, C. D. (2003) *Proc. Nat. Acad. Sci. U.S.A.* **100,** 13196–13201
4. Scott, E. E., He, Y. Q., and Halpert, J. R. (2002) *Chem. Res. Toxicol.* **15,** 1407–1413
5. Williams, P. A., Cosme, J., Sridhar, V., and Johnson, E. F. (2000) *Mol. Cell* **5,** 121–131
6. Yano, J. S., Wester, M. R., Schoch, G. A., Griffin, K. J., Stout, C. D., and Johnson, E. F. (2004) *J. Biol. Chem.* **279,** 38091–38094
7. Williams, P. A., Cosme, J., Vinkovic, D. M., Ward, A., Angove, H. C., Day, P. J., Vonrhein, C., Tickle, I. J., and Jhoti, H. (2004) *Science* **305,** 683–686
8. Scott, E. E., White, M. A., He, Y. A., Johnson, E. F., and Halpert, J. R. (2004) *J. Biol. Chem.* **279,** 27294–27301
9. Scott, E. E., Liu, H., He, Y. Q., Li, W., and Halpert, J. R. (2004) *Arch. Biochem. Biophys.* **423,** 266–276
10. Chen, C. S., Lin, J. T., Goss, K. A., He, Y. A., Halpert, J. R., and Waxman, D. J. (2004) *Mol. Pharmacol.* **65,** 1278–1285
11. Chang, T. K., Weber, G. F., Crespi, C. L., and Waxman, D. J. (1993) *Cancer Res.* **53,** 5629–5639
12. Waller, S. C., He, Y. A., Harlow, G. R., He, Y. Q., Mash, E. A., and Halpert, J. R. (1999) *Chem. Res. Toxicol.* **12,** 690–699
13. Spatzenegger, M., Wang, Q., He, Y. Q., Wester, M. R., Johnson, E. F., and Halpert, J. R. (2001) *Mol. Pharmacol.* **59,** 475–484
14. He, Y. Q., Szklarz G. D., and Halpert, J. R. (1996) *Arch. Biochem. Biophys.* **335,** 152–160
15. Strobel S. M., and Halpert, J. R. (1997) *Biochemistry* **36,** 11697–11706
16. Cherry, J. R. (2003) *Curr. Opin. Biotechnol.* **14,** 438–443
17. Schoemaker, H. E. (2003) *Science* **299,** 1694–1697
18. Schmid, A. (2001) *Nature* **409,** 253–257
19. Kirk, O. (2002) *Curr. Opin. Biotechnol.* **13,** 345–351
20. Turner, N. J. (2003) *Trends Biotechnol.* **21,** 474–478
21. Hult, K., and Berglud, P. (2003) *Curr. Opin. Biotechnol.* **14,** 395–400
22. Farinas, E. T., Schwaneberg, U., Glieder, A., and Arnold, F. H. (2001) *Adv. Synth. Catl.* **343,** 601–606
23. Glieder, A., Farinas, E. T., and Arnold, F. H. (2002) *Nat. Biotechnol.* **20,** 1135–1139
24. Joo, H., Lin, Z., and Arnold, F. H. (1999) *Nature* **399,** 670–673
25. Kim, D., and Guengerich, F. P. (2004) *Biochemistry* **43,** 981–988
26. Kim, D., and Guengerich, F. P. (2004) *Arch. Biochem. Biophys.* **432,** 102–108
27. Harlow, G. R., He, Y. A., and Halpert, J. R. (1997) *Biochim. Biophys. Acta* **1338,** 259–266
28. Cirino, P. C., Mayer, K. M., and Umero, D. (2003) in *Directed Evolution Library Creation* (Arnold, F. H., and Georgiou, G., eds) pp. 3–10, Humana Press, Totowa, NJ
29. Tobias, A. V. (2003) in *Directed Evolution Library Creation* (Arnold, F. H., and Georgiou, G., eds) pp. 11–16, Humana Press, Totowa, NJ
30. Salzar, O., and Sun, L. (2003) in *Directed Enzyme Evolution* (Arnold, F. H., and Georgiou, G., eds) pp. 85–89, Humana Press, Totowa, NJ
31. Scott, E. E., Spatzenegger, M., and Halpert, J. R. (2001) *Arch. Biochem. Biophys.* **395,** 57–68
32. Khan, K. K., Halpert, J. R. (2002) *Chem. Res. Toxicol.* **15,** 806–814
33. Cosme, J., and Johnson, E. F. (2000) *J. Biol. Chem.* **275,** 2545–2553
34. Hilser, V. J., Dowdy, D., Oas, T. G., and Freire, E. (1998) *Proc. Nat. Acad. Sci. U. S. A.* **95,** 9903–9908
35. Hilser, V. J. (2001) *Met. Mol. Biol.* **168,** 93–116
36. Jounaidi, Y., and Waxman, D. J. (2004) *Cancer Res.* **64,** 292–293
37. Chen, L., and Waxman, D. J. (2002) *Curr. Pharm. Des.* **8,** 1405–1416